

Modeling the Global Interannual Variability of Ozone Due to the Equatorial QBO and to Extratropical Planetary Wave Variability

JONATHAN S. KINNERSLEY AND KA-KIT TUNG

Department of Applied Mathematics, University of Washington, Seattle, Washington

(Manuscript received 5 March 1997, in final form 22 September 1997)

ABSTRACT

By forcing an interactive chemical–dynamical model of the stratosphere with the observed Singapore zonal winds and with the observed daily varying planetary wave heights just above the tropopause over the period from March 1980 to February 1993, much of the observed interannual variability (IAV) in the monthly mean ozone column from pole to pole was able to be reproduced. The best correlations were obtained equatorward of 50° during winter and autumn in both hemispheres. These correlations were due to the model's interaction with the specified equatorial zonal wind. In the Southern Hemisphere, the observed high-latitude ozone anomaly in November (the month with the largest anomaly) is well anticorrelated with the 20-mb Singapore wind, and correlations suggest the anomaly propagates poleward from 45°S in August and possibly even from 15°S in June. The model reproduces this behavior well. In the Northern Hemisphere (NH), by contrast, the observed high-latitude ozone anomaly is not well correlated with the equatorial quasi-biennial oscillation nor does it propagate from lower latitudes. Model results demonstrate that the NH high-latitude ozone anomaly is influenced strongly by the IAV in the forcing of the planetary waves. Model results show a large IAV in the ozone column during polar night in the NH (where the Total Ozone Mapping Spectrometer is not able to observe) that is due to the IAV in the forcing of planetary waves.

1. Introduction

There is a significant amount of interannual variability (IAV) in the monthly mean zonal-mean ozone column, and a considerable amount of effort has been spent in trying to understand its causes. While a large part of the variability over the past decade (especially at high southern latitudes) is a negative trend due to the increase in the chlorine loading of the stratosphere, much of it is also due to natural variability and it is important to be able to separate the causes of the observed IAV. This paper will focus on two sources of natural variability: the equatorial quasi-biennial oscillation (QBO) in zonal wind and the variability in the forcing of stratospheric planetary waves at the tropopause. The former has been studied fairly extensively already, using both observations (e.g., Hasebe 1984; Bowman 1989; Lait et al. 1989; Randel and Cobb 1994; Tung and Yang 1994a; Hollandsworth et al. 1995; Randel and Wu 1996; Sitnov 1996) and models (e.g., Gray and Pyle 1989; Gray and Ruth 1993; Tung and Yang 1994b) but the importance of the latter to the ozone column has not yet been quantified, though its effect on

the stratospheric zonal wind in the Northern Hemisphere (NH) was estimated, using an interactive model, by Kinnersley (1998).

The QBO signal in extratropical ozone was at first (e.g., Hasebe 1984; Lait et al. 1989) analyzed without considering in depth the interaction between the tropical QBO and the stratospheric circulation's seasonal cycle. Subsequently, the seasonal synchronization of the subtropical ozone QBO anomaly was noted by Bowman (1989) and Hamilton (1989) and modeled by Gray and Dunkerton (1990) and Gray and Ruth (1993) using a two-dimensional model. In addition, Tung and Yang (1994a) highlighted the fact that the mid- and high-latitude ozone variability seemed to involve an interference between the approximately 30-month tropical QBO and the 12-month seasonal cycle. They used a simplified model (Tung and Yang 1994b) to demonstrate their results and assumed that the tropical QBO somehow modulated the extratropical planetary wave forcing in winter [as suggested in earlier studies by Holton and Tan (1982) and Dunkerton and Baldwin (1991)] and hence the meridional circulation, so that the extratropical ozone variation was mainly a manifestation of the circulation anomaly in the extratropics. In their model the extratropical anomaly in column ozone was created locally, with high column ozone in regions of enhanced downward transport and low column ozone in regions of enhanced upwelling. This is a different and perhaps complimentary view to the one suggested by Gray and

Corresponding author address: Dr. Jonathan S. Kinnersley, Department of Applied Mathematics, University of Washington, Box 352420, Seattle, WA 98195-2420.
E-mail: jsk@amath.washington.edu

Pyle (1989), who modeled an extratropical QBO in ozone by a poleward advection and diffusion of the tropical anomaly. It would be useful to use a more realistic model with an interaction between planetary waves and the mean flow to see to what extent the observed extratropical ozone anomaly can be reproduced. Also, a more complicated model would be able to use the information contained in the tropical wind at all levels, rather than assuming that the tropical QBO can be represented simply by the wind at a single pressure level, as has been done in previous observational and modeling studies [though Randel and Wu (1996) found that a linear combination of the Singapore winds was better correlated with the observed ozone column than the wind at a single level]. Such a modeling approach was taken previously by Gray and Ruth (1993), but their model did not simulate the interaction between planetary waves and the zonal-mean wind. Chipperfield et al. (1994) used a model (an earlier version of the model used in this study) with such an interaction, but little attention was paid to the extratropical variability.

In the SH, a strong QBO signal has been found at high latitudes (e.g., Garcia and Solomon 1987; Lait et al. 1989; Randel and Cobb 1994). The high-latitude NH QBO signal is, however, weaker than that of the SH (see, e.g., Randel and Cobb 1994; Tung and Yang 1994a). It is probable that variability in planetary wave forcing from the lower stratosphere in the NH (which may be influenced by a number of factors, such as wave propagation from the troposphere or the equatorial QBO) is important to the high-latitude ozone column variability. That it is important to the variability of the 10-mb zonal winds was demonstrated by Kinnersley (1998) using the same model as in this paper. It might be difficult to find a quantity related to the wave activity in the lower stratosphere that is well correlated with the high-latitude ozone column variability. Also, merely finding correlations would not demonstrate a causal link, but only suggest it. An alternative to looking for correlations is to feed the planetary wave amplitudes observed just above the tropopause into an interactive model that is able to calculate the resultant planetary waves throughout the stratosphere as well as their interaction with the zonal-mean state and estimate the resultant variability induced in the ozone column. That is the approach taken in this study, with waves on the 368-K isentropic level being used (which lies near the 150-mb surface just above the extratropical tropopause).

The model and data used here will be described in section 2. Then in section 3 the correlation of the observed ozone column with the Singapore wind will be presented and discussed with respect to previous studies. The model runs will be presented in section 4, and the results will be discussed in the concluding section.

2. Model, data, and statistics

a. Model

The model used here is the "THIN AIR" (Two and a Half dimensional Inter-Active Isentropic Research)

model with zonally truncated dynamics and zonally averaged chemical and radiative modules. It is described fully in Kinnersley (1996). It has 19 horizontal boxes from pole to pole and 29 levels in the vertical, from the ground to about 100 km. It uses an explicit Adams–Bashford time-integration with a step of 2 h. However, unlike the model version used in Kinnersley (1996), in the version used here the planetary wave breaking parameterization has been replaced by a meridional diffusion of wave potential vorticity with a constant diffusion coefficient that damps two-grid-length scale anomalies with an e -folding time of about 10 days. Also, the planetary waves were damped within 27° of the equator with a time constant of 1.5 days since it was shown in Kinnersley (1998) that this led to a better simulation of the interannual variability in the zonal wind during late winter in the NH. Similar results were obtained using the original breaking parameterization, but it was decided to use the simpler scheme here to show that the results do not depend strongly on the kind of wave breaking parameterization used. The meridional diffusion coefficient for trace gases in the model is parameterized by the flux gradient method of Tung (1986) and Yang et al. (1990) and depends on the ratio of Ertel's potential vorticity (PV) flux to the meridional gradient of the zonal-mean PV. This method assumes that the main cause of a nonzero time-averaged PV flux is a meridional diffusion of eddy PV. This is indeed true for this model, so it seems appropriate to use it here. This method has the following limitation, however. Provided the zonal-mean meridional PV gradient is positive (which is true most of the time) the method results in a diffusion coefficient whose sign is opposite to that of the PV flux. A reversible wave vacillation will result in negative and positive PV fluxes as the wave grows and then decays, and hence positive and negative values of diffusion coefficient. Over the whole vacillation the net diffusion should be zero (if the vacillation is reversible). However, the problem with this method is that it will overestimate the diffusion for the simple reason that the numerical model cannot handle negative diffusion coefficients and has to set them equal to zero. This problem would not be so acute if the time-mean diffusion were parameterized in terms of the time-mean PV flux [as was done in Yang et al. (1990), for example], but that cannot be done in this model, which computes the daily evolution of the stratosphere. With this in mind, extra model runs were carried out, one with this parameterized diffusion and one with zero diffusion so that the uncertainty in the modeled results might be quantified. The results obtained while using the parameterized diffusion were very similar to those obtained while using no diffusion, but were, in general, more realistic. Therefore, only results from the runs with diffusion will be discussed in this paper.

A simple gravity wave parameterization helps to produce realistic upper-stratospheric and mesospheric winds and also determines the vertical diffusion of trace

gases in the stratosphere using Lindzen's (1981) technique. Near the tropopause a value of $1 \text{ m}^2 \text{ s}^{-1}$ is used to represent cross-tropopause diffusion.

The planetary wave module solves the quasigeostrophic system of equations for the three longest zonal wave components (i.e., it integrates the prognostic equations for the wave components of Ertel's PV using the geostrophic winds derived by inverting PV at each time step) and includes wave-wave interactions as well as interactions with the modeled zonal-mean state. Its bottom boundary is the 368-K isentropic surface (which lies near 150 mb) and its waves are forced there with the observed daily wave heights expressed in terms of the Montgomery potential. For the runs described in this paper, with the exception of one control run, the model's planetary waves in the NH were forced at the 368-K isentropic surface using the observed planetary wave amplitudes from March 1980 to February 1993. In the SH the forcing of the waves on the 368-K surface was annually periodic (using the daily varying data from July 1980 to June 1981) since use of the observed interannually varying waves gave unrealistic results in the modeled SH. This may be due to errors in the observations, which rely on a sparse set of observations of surface pressure in the SH to build up the geopotential height data throughout the atmosphere. In addition, with the exception of a second control run, the zonal winds in the model between 10 and 70 mb and equatorward of 10° N and S were relaxed toward the observed Singapore wind with a time constant of 1 day, similar to Chipperfield et al. (1994).

Holton and Mass (1976) suggested that the stratosphere may be chaotic, even with a constant forcing from the troposphere, but it was shown in Kinnersley (1998) that the model used here is not chaotic in this way.

b. Data

The ozone values came from the Total Ozone Mapping Spectrometer (TOMS) dataset (version 7) from November 1978 to April 1993. The ozone data was detrended using a least squares fit to determine the trend. The daily planetary wave heights used to force the model's waves were derived from National Meteorological Center (now the National Centers for Environmental Prediction) data from March 1980 to February 1993.

c. Statistics

The correlations shown throughout this paper are all calculated from monthly mean values. The significance of the correlations was estimated in the following simple way. The correlation between, for example, the observed and modeled anomalies in the monthly mean ozone column at a certain latitude from 1980 to 1992 involves 13 pairs of numbers. With 13 pairs of random numbers, the probability of obtaining a correlation co-

efficient greater than 0.48, 0.64, and 0.79 is 0.05, 0.01, and 0.001 respectively. This is expressed in this paper by saying that correlations of 0.48, 0.64, and 0.79 obtained over 13 years are significant at the 95%, 99%, and 99.9% levels respectively. The standard deviations referred to in the text are the standard deviations of the monthly mean, zonal-mean value from the average value (over the entire data record) for that month.

3. Correlation of ozone column with Singapore wind

A number of methods have been used to isolate a signal in the global ozone column, which is correlated with the equatorial QBO in stratospheric zonal wind. Chandra and Stolarski (1991) showed the correlation between the 30-mb Singapore wind and the TOMS ozone column from 60° S to 60° N and for each month of the year and also calculated a regression coefficient. This revealed the seasonal dependence of the QBO signal in ozone, which was clearly strongest during winter and autumn. Bowman (1989), Hollandsworth et al. (1995), and Sitnov (1996) calculated lagged correlations and anomalies of ozone with the Singapore wind at a certain level, with positive and negative lags of up to 2 years. While these revealed a significant QBO signal even at high latitudes, they hid its seasonality.

Since we are interested here in the seasonality of the extratropical ozone QBO, the zero-lagged correlation of the detrended TOMS ozone column from March 1980 to February 1993 with the 20-mb Singapore wind is shown in Fig. 1a. The 13-yr time span used here is shorter than the total TOMS record, but it is used in order to be able to compare it with the model results. However, there is no reason to suppose that the extratropical QBO signal should depend solely on the Singapore wind at one particular level, and Randel and Wu (1996) found a linear combination of the Singapore winds from 10 to 70 mb that provided a better fit to the ozone variability than the wind at a single level. Therefore, for comparison, the correlation with Randel and Wu's (1996) linear combination of winds (in which the 20-mb wind received the strongest weighting) is shown in Fig. 1b. Although use of the linear combination of winds does give slightly better results over the equator and near 45° N from November to April, on the whole the results are very similar to those obtained using the 20-mb wind alone. Strong correlations in Fig. 1 are obtained near the equator for all months of the year, consistent with theory and previous studies. There is a node at about 10° N and S where the correlation with the equatorial wind changes sign. In the SH there is a strong negative correlation that starts in March and extends from about 10° to 30° S and then grows in width until it extends from 10° S to about 50° S in October. In the NH the correlation is again strongest in winter and spring but is not as strong as in the SH, nor does it spread with time away from the Tropics. It also starts

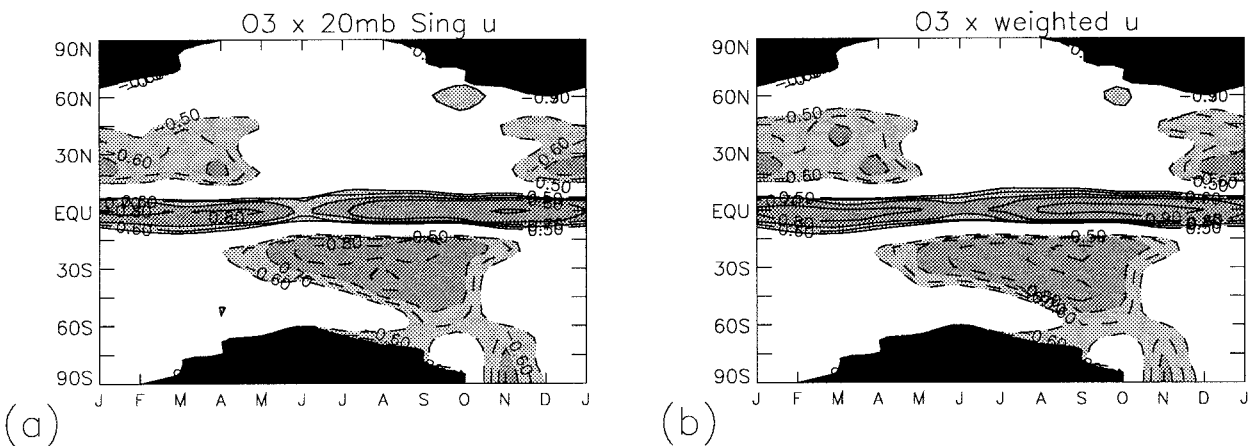


FIG. 1. Correlation of observed ozone column anomaly (detrended and deseasonalized) from March 1980 to February 1993 with (a) the 20-mb Singapore zonal wind and (b) with Randel and Wu's (1996) linear combination of the Singapore winds. Contours at ± 0.5 , ± 0.6 , . . . ; negative contours dashed; absolute values greater than 0.5 lightly shaded; absolute values greater than 0.7 more heavily shaded. The polar night is blacked out.

later in the seasonal cycle, in early winter as opposed to late autumn in the SH.

The NH high-latitude (north of 50°N) winter and spring ozone column does not seem to be strongly influenced by the Singapore winds. However, in the SH in November there is a significant high-latitude ozone column modulation by the 20-mb Singapore wind. This interhemispheric difference (a weaker NH QBO signal) is also present in Randel and Cobb's (1994) results. This is the opposite of what was found by Hollandsworth et al. (1995), who saw a stronger QBO signal at NH high latitudes than at high latitudes in the SH. Although the difference is presumably due to the latter's use of lagged correlations, it is not clear to us why the difference arises.

From Fig. 1 it seems that the SH ozone column anomaly may be propagating from low latitudes in June to high latitudes in November, while such a propagation is not evident in the NH. This difference between the

NH and SH at high latitudes can be further revealed by calculating the correlation between the high-latitude ozone column anomaly of a certain month and the low-latitude ones over the preceding 12 months. The standard deviation of the monthly mean ozone column at 60°S is largest in November and at 60°N it is largest in February (Fig. 2), so these are the two high-latitude points we shall use. The correlation between the anomaly at 60°S in November and the anomaly at every latitude over the preceding 12 months (Fig. 3a) suggests a strong propagation of the anomaly from 15°S in June (correlation of 0.6) to 45°S in August (correlation of 0.8) and eventually to 60°S in November. If the anomalies at these three points in time and latitude were random, the chance of finding correlations of 0.64 and 0.79 would be 1% and 0.1% respectively, so it would seem that these anomalies are not random but are linked together, possibly by poleward advection or diffusion. The corresponding calculation for the NH (Fig. 3b), correlating the anomaly at 60°N in February with that over the preceding 12 months, suggests no propagation of the anomaly from lower latitudes. This is consistent with the work of Yang and Tung (1995), who found no phase propagation of the ozone QBO in the NH.

It will be argued in section 4 that the weaker NH high-latitude QBO signal found in this study and the isolation of the NH winter high-latitude ozone anomaly are due to the disruption of the QBO signal by the variability in the forcing of the NH planetary waves.

4. Results of model runs

Three model runs will be presented in this section. In run A the model is forced both by the equatorial Singapore winds from 10 to 70 mb and by the observed NH wave amplitudes on the 368-K isentropic surface from March 1980 to February 1993. In the SH the forc-

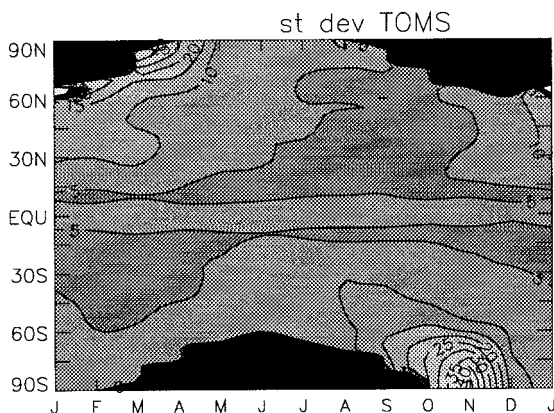


FIG. 2. Standard deviation of the observed ozone column anomaly (detrended and deseasonalized) from March 1980 to February 1993 (contours every 5 DU).

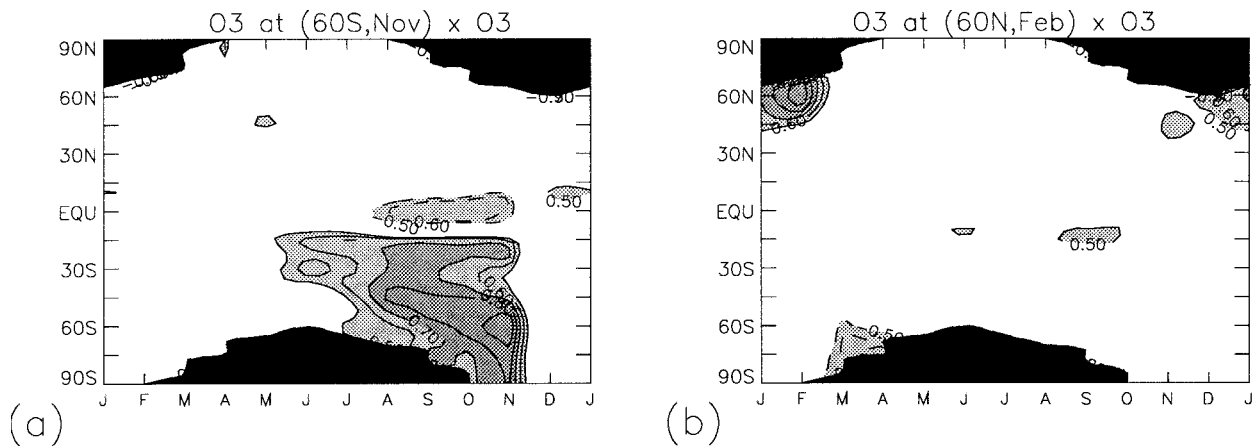


FIG. 3. (a) Correlation of observed ozone column anomaly (detrended and deseasonalized) at 60°S in November with observed anomaly at all latitudes over the preceding 12 months. (b) As in (a) but using the anomaly at 60°N in February. Contours and shading as in Fig. 1.

ing of the waves on the 368-K surface was annually periodic (see section 2). The model was initialized using the March values from the final year of a 12-yr run where the forcing of the model's planetary waves at the 368-K surface was made annually periodic in both hemispheres by repeating the observed wave heights from July 1980 to June 1981. Two control runs, in which these two forcings were applied separately, will be described in sections 4b and 4c.

a. Run A—With equatorial QBO and variable forcing of NH planetary waves

The model was run as described above for 13 yr using the observed forcings from March 1980 to February 1993.

The performance of the model was shown in Kinnersley (1996) to be very realistic in a number of ways, but since the model is slightly different in this study and is run with forcings that vary from year to year, the 13-yr average of the modeled and observed ozone col-

umns are shown for comparison in Fig. 4. The model generally compares well with observations when it is taken into account that the chlorine loading in the model is held close to the value estimated for 1980. The model is therefore unable to reproduce the severe ozone losses observed after 1985 at the South Pole in October.

For comparison with Tung and Yang (1994b), and for a general picture of the model's performance, the modeled and observed ozone columns at certain latitudes for each month from January 1982 to December 1992 are plotted in Fig. 5. In general, the model is quite close to observations. At 60°N the modeled anomaly is somewhat larger than observed—this will be discussed later. Also, the model's anomalies tend to spread over a wider latitude range than observed. For example, the modeled positive anomaly at 20°S in mid-1989 travels to 60°S in late 1989 and even grows, whereas the observed anomaly at 20°S is not apparent at 40° or 60°S. This is more evident in the contour plot of both anomalies (see Fig. 6), where the smoothness of propagation of the modeled SH anomaly is contrasted with the much more

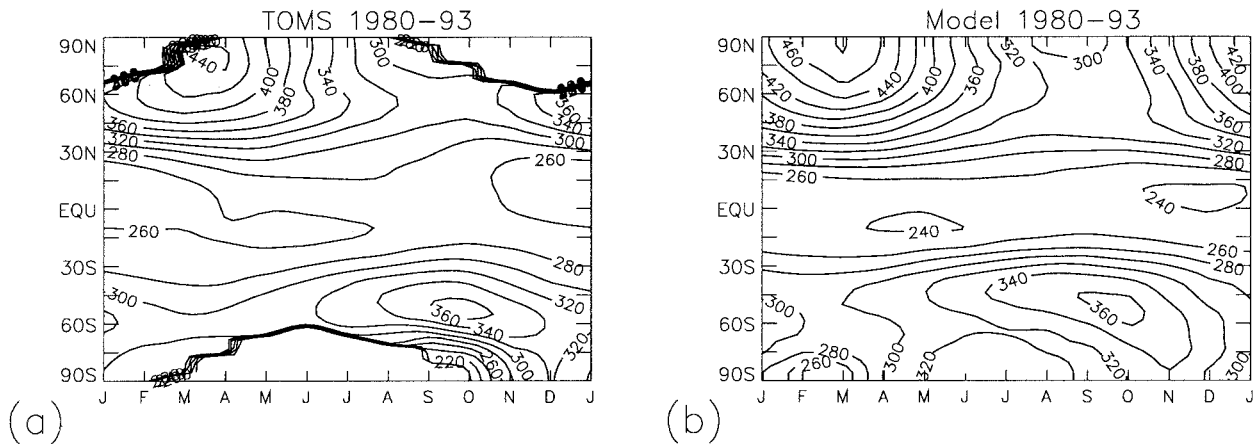


FIG. 4. 13-yr average (1980–92) of ozone column (a) from TOMS data and (b) from model.

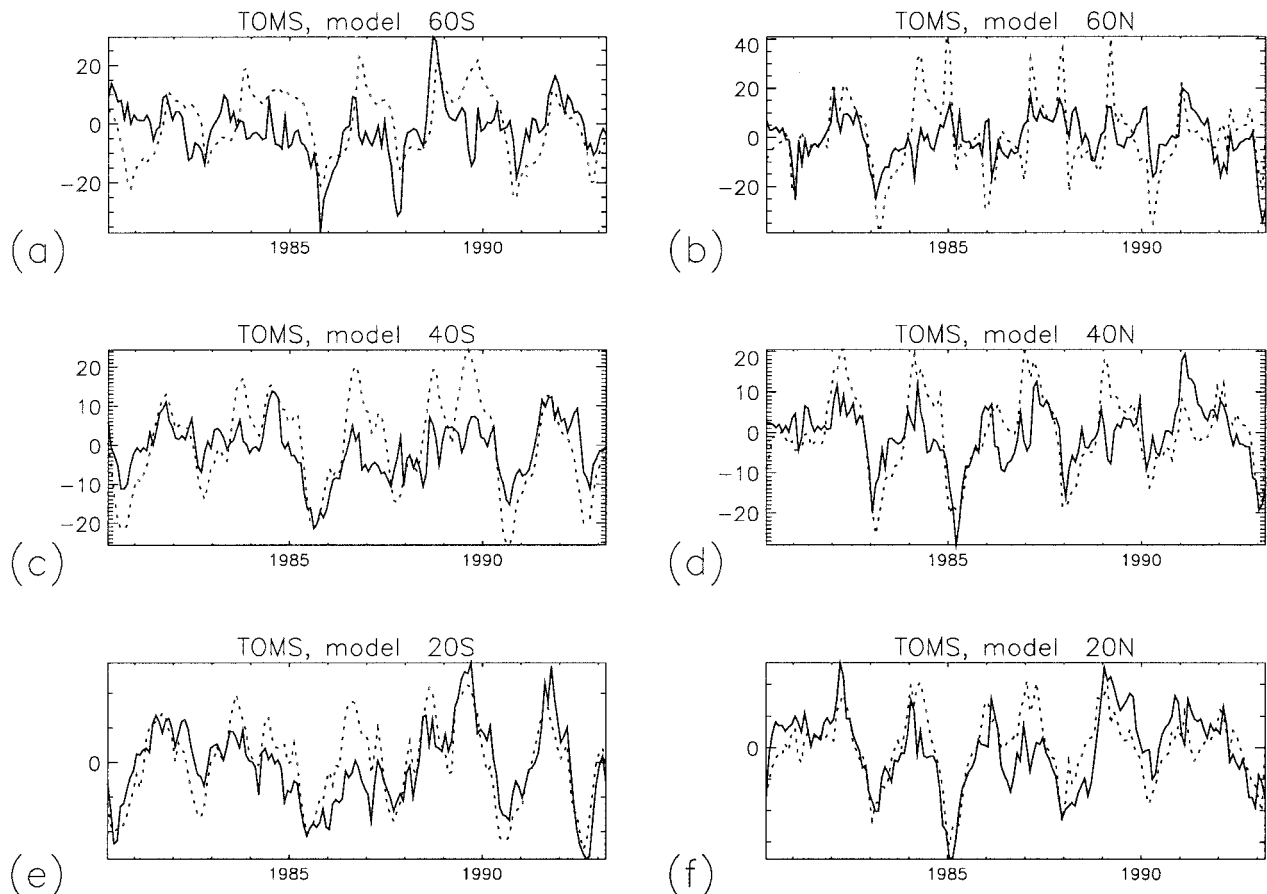


FIG. 5. Comparison of modeled (dashed) and observed (solid) ozone column anomalies (detrended and deseasonalized) from Mar 1980 to Feb 1993 at (a) 60°S, (b) 60°N, (c) 40°S, (d) 40°N, (e) 20°S, and (f) 20°N.

noisy TOMS data. Yang and Tung (1995) noted that the observed ozone column in the NH changes sign near 55°N during some winters. They speculated that this may be caused by interannual variability in the high-latitude planetary waves, since they were unable to reproduce the sign change in their simple model incorporating only equatorial QBO variability. This feature is now reproduced in the NH of this model (see Fig. 6), in particular in the early winters of 1984/85, 1987/88 and 1991/92, though a better comparison is hindered by lack of observations during polar night. It must be borne in mind that the model's horizontal resolution of 9° limits the precision of the comparison. Note also that the model's NH is more noisy than the SH due to the interannual variability in the 368-K wave heights in the NH. This makes the model's NH look more realistic than its SH and suggests that, although the model mimics the observed SH ozone anomaly well in general (see below), interannual variability in the SH planetary wave forcing at a level in the lower stratosphere may be the cause of the observed noise in the SH ozone column anomaly. The polar night regions have been blacked out in the model results for an easier comparison with TOMS data. The depletion of ozone during the NH win-

ters of 1991/92 and 1992/93 in the TOMS data [analyzed by Randel et al. (1995), among others] is evident from a comparison between modeled and observed anomalies.

The correlation of modeled with observed ozone anomalies shown in Fig. 7a is a critical test of the model since the correlation is calculated at each latitude and month over the 13-yr interval. As expected, the correlation is strong equatorward of 10° since the model zonal winds are specified from observations there. It is also strong between about 10° and 50° in both hemispheres during their respective winters and springs, which is when the wave-induced poleward circulation is strong. The model's variability at midlatitudes (see Fig. 7b) is somewhat larger than observed, however. The reason for this is at present unclear.

In the NH, the correlation between the high-latitude modeled and observed ozone column anomalies is good (exceeding 0.6) for most months of the year when the anomaly is large. It will be shown in section 4c that this correlation is due to a combination of the effect of the equatorial QBO and the IAV in the forcing of the planetary waves at 368 K. Note that the model produces a large IAV in the ozone column during polar night

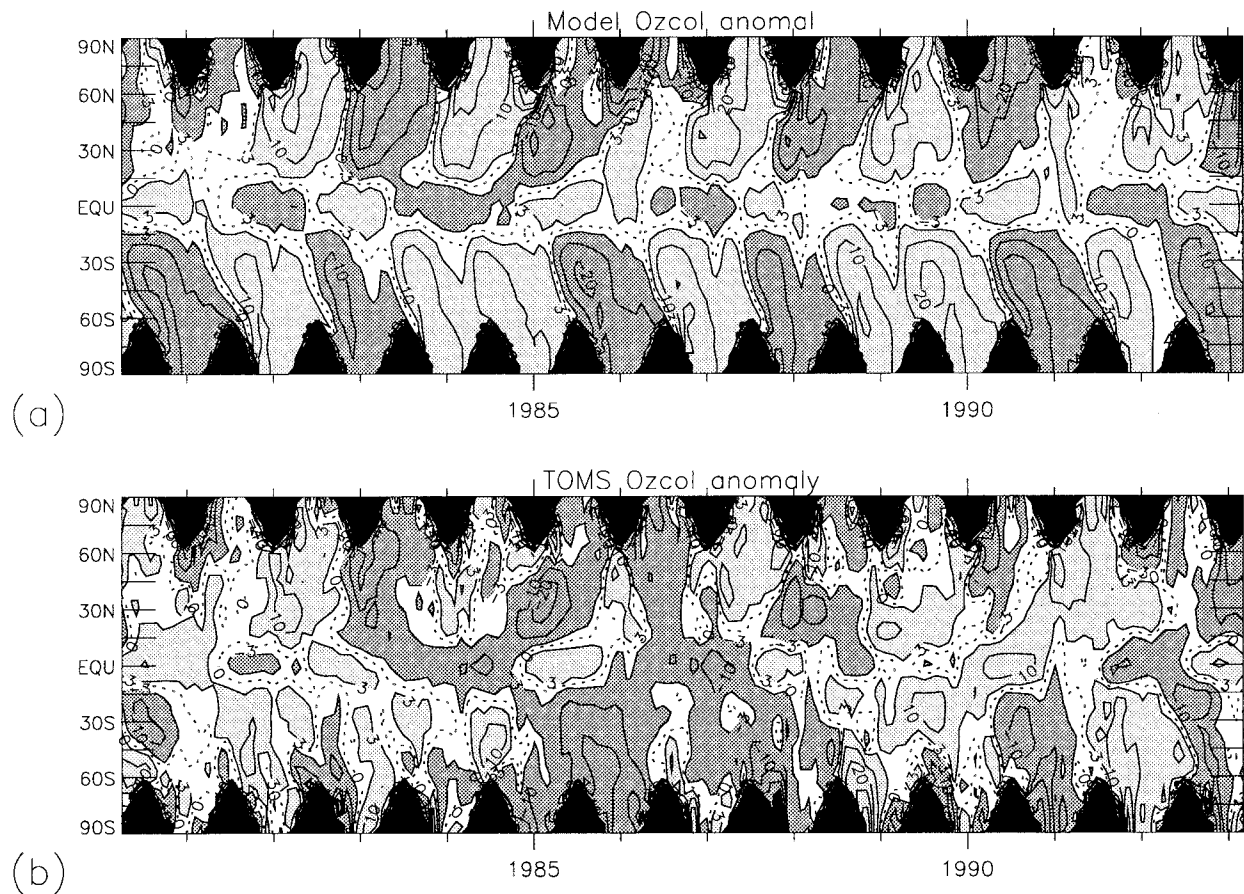


FIG. 6. Ozone column anomaly from (detrended and deseasonalized) (a) full model and (b) TOMS data. Contours at 0, ± 3 , ± 10 , ± 20 , ± 40 , ± 60 DU. Values above 3 shaded.

(Fig. 7b), which is when TOMS is unable to measure the ozone column. A high variability during polar night is perhaps not surprising since ozone has a very long chemical lifetime then and will be strongly affected by

variability in the dynamics of the NH, which is large during winter.

In the SH at high latitudes the correlation is strong (over 0.6, which is near the 99% significance level)

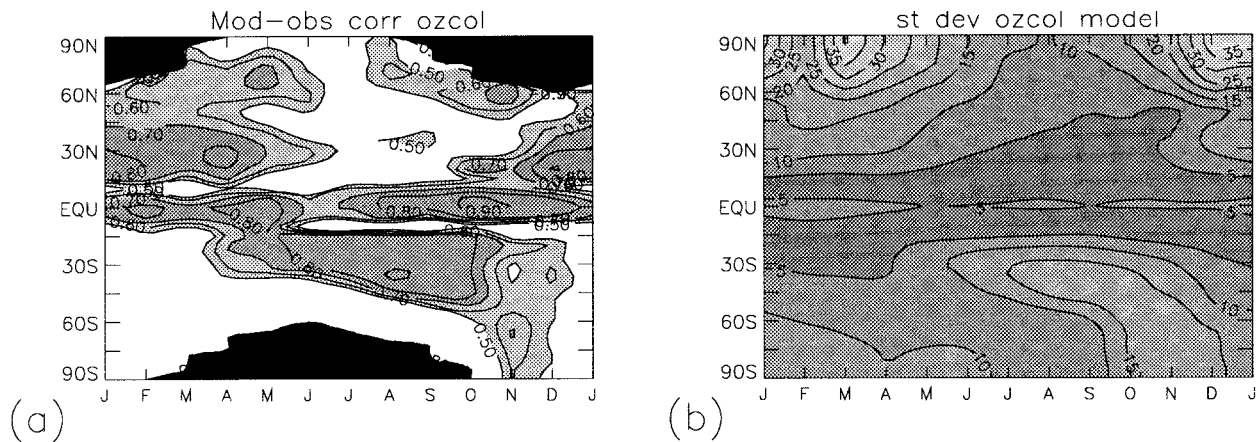


FIG. 7. (a) Correlation of modeled and observed ozone column anomalies (detrended and deseasonalized) from Mar 1980 to Feb 1993. Contours and shading as in Fig. 1. (b) Standard deviation of the modeled ozone column anomaly.

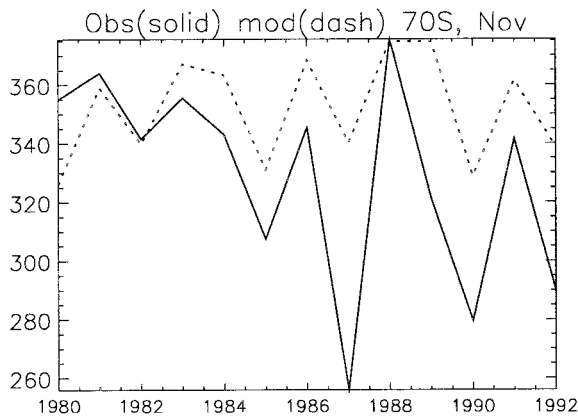


FIG. 8. Nondetrended TOMS (solid) and modeled (dashed) ozone column at 70°S in November.

during November, which is the time of greatest ozone column variability there. The modeled variability (Fig. 7b) is less than observed, however. The large variability observed may be due to the presence in the real atmosphere of the “ozone hole,” which is not simulated by the model (since it maintains the chlorine loading representative of 1980). From Fig. 8 (in which the TOMS data has not been detrended) it can be seen that the model’s variability at 70°S in November is very similar to that observed until 1985. After 1985 the negative anomalies observed in 1987, 1990, and 1991 have a much stronger negative trend than the more positive anomalies of 1986, 1988, and 1991. This suggests that a positive feedback amplifies the negative anomalies, perhaps in the following way. If the southern pole becomes colder than usual due to the QBO, there will be more ozone depletion (if the chlorine loading is high) due to enhanced polar stratospheric cloud formation. This will lead to reduced solar ozone heating, a stronger vortex, a decrease in planetary wave activity, and so less mixing of ozone from lower latitudes, which will further reduce ozone values.

As a comparison with Fig. 1a, the correlation coefficient between the modeled ozone column anomaly and the 20-mb Singapore wind was calculated. In general, the modeled correlations (Fig. 9) are stronger than observed. The anticorrelation of the high-latitude SH anomaly with the 20-mb Singapore wind is reproduced, though in the model it is strongest in October, while the observed anticorrelation is strongest in November. Since the equatorial ozone anomaly in the real atmosphere must depend on the zonal wind at all longitudes and over a band of latitudes within about 10° of the equator, and not just on the wind over Singapore, while the modeled ozone is modulated by the Singapore wind, it is not surprising that the model is better correlated than observations with the Singapore wind. Figure 9 does show, though, the regions and times at which the modeled ozone anomaly is very sensitive (with correlations exceeding 0.9) to its 20-mb equatorial zonal-mean zonal

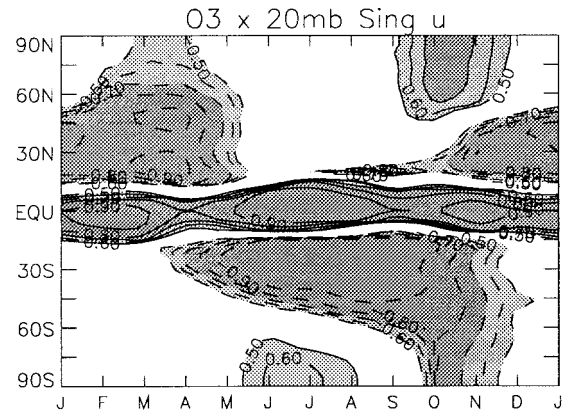


FIG. 9. As Fig. 1a but using modeled ozone column.

wind. The model also reproduces the positive correlation seen in Fig. 1a near 60°N in October, which seems (see Fig. 13 and discussion in section 4b) to be a remnant of the spring anomaly at 30°N. Note also that the correlations at northern high latitudes in spring are lower than those during spring at southern high latitudes. This is because of the added variability in the NH due to the variability in the forcing of planetary waves.

The vertical structure of the ozone variability has been studied using SAGE II data by Zawodny and McCormick (1991), and Randel and Wu (1996). The vertical structure of the standard deviation of the modeled monthly mean ozone density (in DU/km) from its climatological value is shown in Fig. 10. Over the equator between 20 and 30 km the variability reaches about 1 DU/km, which is very close to the value observed by Randel and Wu (1996), though between 30 and 35 km the value is about a third of that observed. This is due to the model’s poor simulation of the upper stratospheric QBO (which will not be described here). At 30°N and 30°S near 20 km there are peaks in the ozone density variability, as observed by Randel and Wu (1996), though the variability near 30 km is again less than

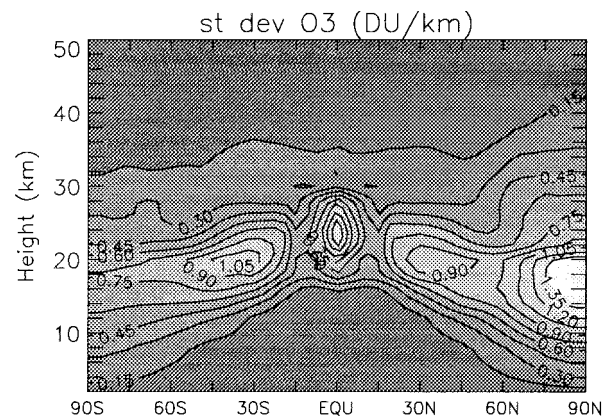


FIG. 10. Standard deviation from the monthly climatology of the modeled ozone density (in DU/km).

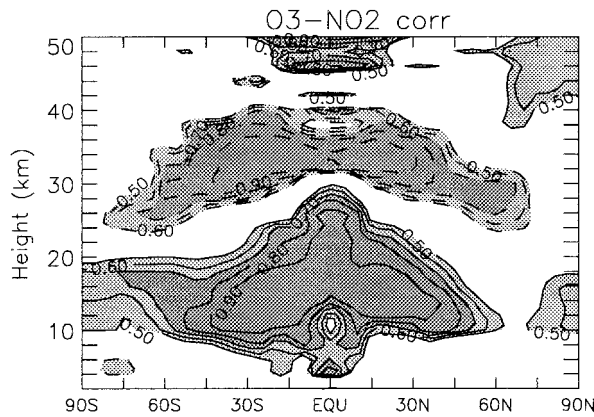


FIG. 11. Correlation of modeled ozone and NO₂ anomalies. Contours and shading as in Fig. 1.

observed. At high northern latitudes there is a large variability from the troposphere to the middle stratosphere.

As has been pointed out by several authors (e.g., Chipperfield et al. 1994; Randel and Wu 1996), ozone in the middle stratosphere is chemically determined, mainly by the concentration of NO₂, with larger values of NO₂ causing lower ozone values. As a comparison with Randel and Wu's Fig. 18, Fig. 11 here shows the modeled correlation between monthly mean ozone and NO₂ over all months of the 13-yr model run. This involves 156 months, but if ozone or NO₂ anomalies persist for about 3 months then we estimate about 50 degrees of freedom. In that case, the 99.9% significance level lies at a correlation of 0.4, so it can be seen that there is a strong anticorrelation between NO₂ and ozone over the equator between about 30 and 40 km extending poleward to about 60°N and 60°S between 25 and 30 km. The line of zero correlation is plotted in Fig. 10, from which it can be seen that the majority of the ozone anomaly lies below it in the dynamically controlled (for ozone) region, while a smaller part of the anomaly (per-

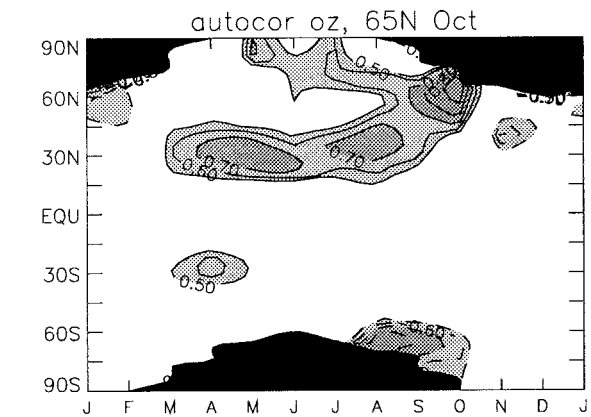


FIG. 13. Correlation of observed ozone column anomaly (detrended and deseasonalized) at 65°N in October with observed anomaly at all latitudes over the preceding 12 months. Contours and shading as Fig. 1.

haps a quarter of it) lies in the chemically controlled region. The chemically controlled part is therefore slightly smaller than Randel and Wu's estimate of a third, using the SAGE II data.

b. Equatorial QBO-only run

In order to isolate the effect of the equatorial zonal wind, the model was run with the tropical winds relaxed toward the observed Singapore wind, as in the previous run, but with an annually periodic planetary wave forcing at the 368-K isentropic surface (using the July 1980–June 1981 values repeatedly). This is similar to the method used by Gray and Pyle (1989), Gray and Ruth (1993), and Chipperfield et al. (1994).

The correlation between modeled and observed ozone column (Fig. 12a) south of about 50°N is very similar to that of run A (Fig. 7), which shows that the ability of the model to simulate the low- and midlatitude (and also the SH November high latitude) ozone anomaly is

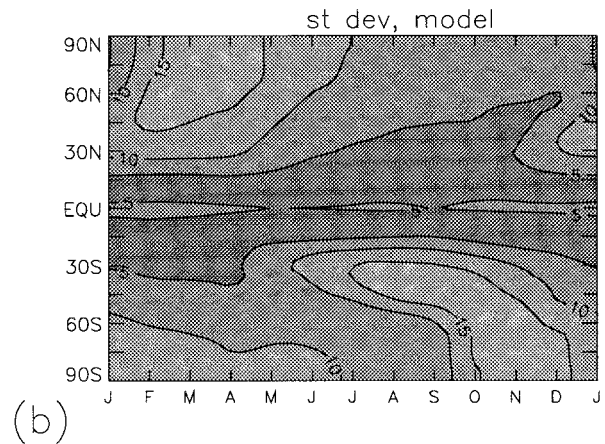
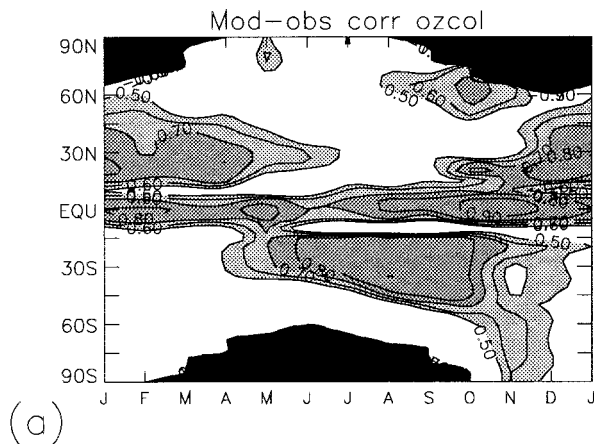


FIG. 12. As in Fig. 7 but for model run with variation of equatorial winds only (section 4b).

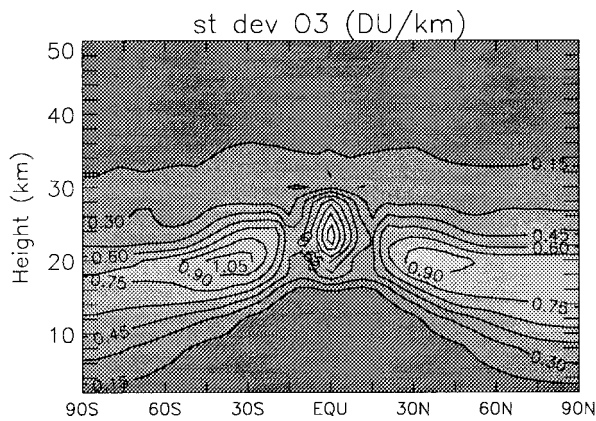
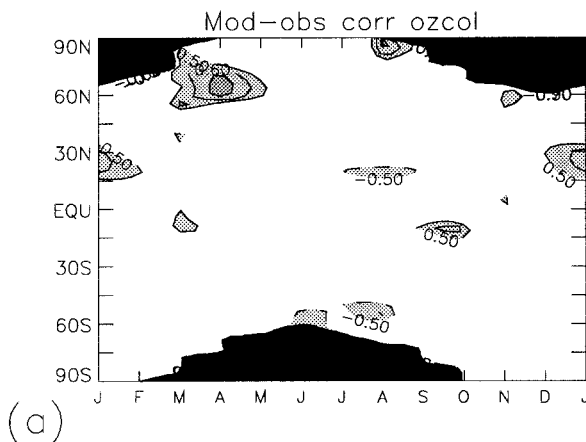


FIG. 14. As in Fig. 10 but for model run with variation of equatorial winds only (section 4b).

due to the forcing of the equatorial QBO. North of 50°N , but only from September to November, the model is well correlated with observations (as it was in run A). Thus, the QBO does appear to play a part in the high-latitude NH ozone anomaly, but only in the autumn. However, this anomaly does not appear to be connected in the usual way to the equatorial wind in autumn—in Fig. 1a there is a region of *correlation* between the 20-mb Singapore wind and the October ozone anomaly at 60°N , as opposed to the expected anticorrelation. The anomaly in October appears to be a remnant of the subtropical NH spring anomaly, as revealed by Fig. 13, which shows the correlation of the observed October anomaly at 65°N with the anomaly over the preceding 12 months. The subtropical spring anomaly appears to persist through summer at low latitudes and then to move poleward during autumn.

The modeled anomaly (Fig. 12b) is also very similar to that of run A south of 50°N , but farther north the anomaly is much smaller than that of run A during winter and reaches a maximum in spring of about half the value of run A.



(a)

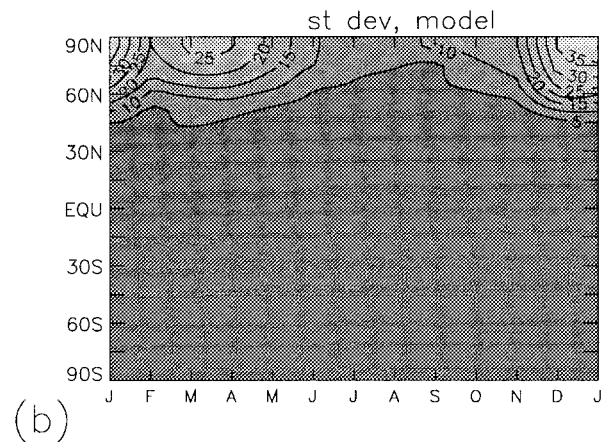
The vertical structure of the ozone anomaly in this QBO-only run (Fig. 14) is very similar to that of run A except at high northern latitudes where the anomaly is smaller in general (about half of the total) and particularly above about 25 km. This will be discussed further in the following subsection.

c. Run with IAV in forcing of planetary waves only

In order to isolate the ozone variability due to the varying forcing of planetary waves, a second control run was performed that was identical to run A except that no equatorial QBO forcing was applied and the model was allowed to calculate its own equatorial winds.

The size of the anomaly in the modeled ozone column from this run (Fig. 15b) is small south of 40°N , but north of about 60°N it is very similar to that of run A. The correlation between modeled and observed ozone column (Fig. 15a) is fairly strong near 60°N from March to May and in November, though unfortunately polar night obscures TOMS data in the region where most of the modeled variability lies. Note, however, that the strong correlations with observations north of 60°N in January and February apparent in run A (Fig. 7) do not occur in this model run. It seems that the total anomaly is, therefore, a combination of the anomalies produced by the QBO and the variability in the forcing of planetary waves. This is confirmed by Fig. 16 in which the anomalies at 65°N in February are plotted for all three runs. It can be seen that the good agreement produced by run A in 1986, for example, is due mainly to the anomaly produced by the planetary wave variability, while in 1987 it is due mainly to the QBO.

The vertical structure of the anomaly (Fig. 17) shows that the discrepancy between the anomalies of run A (Fig. 11) and the QBO run of section 4b (Fig. 15) is due, not surprisingly, to the variability in the forcing of planetary waves. Figures 14 and 17 show similar values



(b)

FIG. 15. As in Fig. 7 but for model run with year-to-year variation of 368-K planetary wave heights only (section 4c).

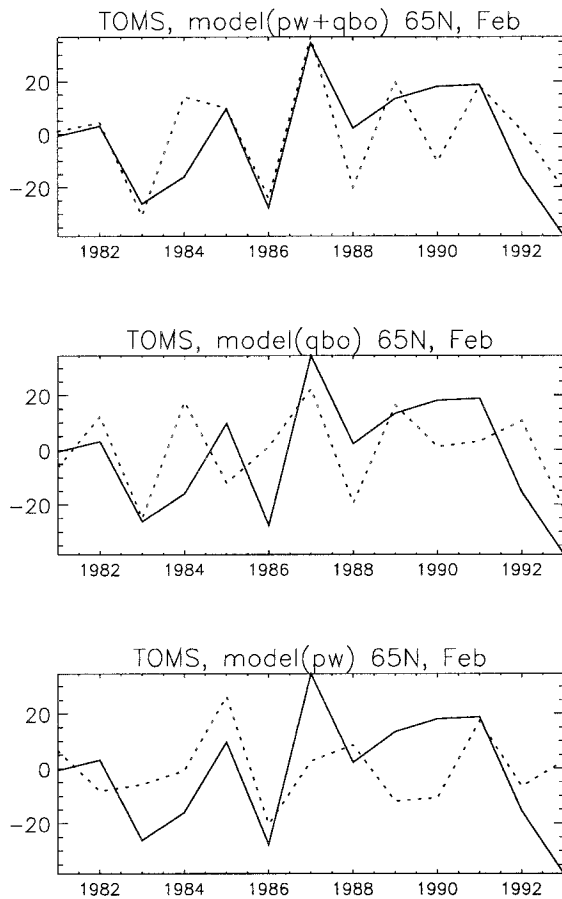


FIG. 16. Observed (solid) and modeled (dashed) ozone column anomalies at 65°N in February from (a) run A, (b) run with variation of equatorial winds only (section 4b), and (c) run with variation of 368-K planetary wave heights only (section 4c).

in the high-latitude troposphere, but above 20 km the high-latitude anomaly due to variability in the forcing of planetary waves is much larger than that due to the equatorial QBO. This is presumably because the planetary waves affect the high northern latitudes strongly during winter when the high-latitude ozone at all heights is dynamically controlled.

5. Discussion and conclusions

It has been shown that much of the ozone variability between about 50°N and 50°S can be accounted for by the effect of the equatorial winds on the extratropical circulation (though a detailed investigation of the mechanism will be described in a later paper). This is consistent with previous observational studies (e.g., Randel and Wu 1996). Observational results shown here suggest that the ozone column anomaly produced in June near 15°S propagates southward past 45°S in August to reach the South Pole in November. The model shows a similar propagation of the SH subtropical autumn anomaly (which is induced mainly by the equatorial 20-mb zonal

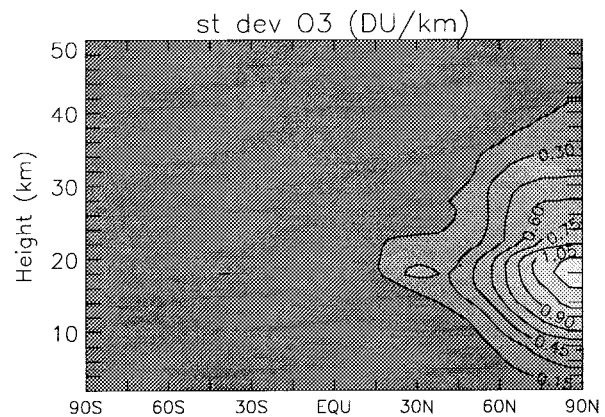


FIG. 17. As in Fig. 10 but for model run with year-to-year variation of 368-K planetary wave heights only (section 4c).

wind) toward the South Pole, though it reaches the pole in October, slightly earlier than observed. The model, therefore, contains a mechanism capable of producing a realistic propagation of the anomaly, and analysis of this mechanism will be presented in a later paper. One striking difference between the modeled and observed anomalies is the rapid growth of the observed SH anomaly (see Fig. 2) as it nears the South Pole, while the modeled anomaly is larger than observed at midlatitudes but maintains a fairly constant amplitude as it nears the pole. The growth of the observed anomaly may be due to the presence in the stratosphere of large concentrations of chlorine after 1985, which may amplify the negative ozone QBO anomalies at high latitudes (see section 4). Figure 18 shows the amplitude of the observed ozone anomaly in the seven years before (Fig. 18a) and after (Fig. 18b) January 1986. (Note that the trends have been removed from the data in Fig. 2 and 18, so they do not contribute to the amplitude of the anomaly). Before 1986 the size of the anomaly in the SH is much closer to that modeled (see Fig. 7b and note that the chlorine loading in the model is typical of that in 1980) while after 1986 the anomaly over the South Pole has increased about threefold and now reaches a maximum in November as opposed to October. Interestingly, the anomaly in the NH is also larger during the later period, perhaps indicating that a similar process is occurring there. This is an interesting result but obviously far from conclusive.

In the NH, the interannual variability in planetary wave forcing from the lower stratosphere has a large effect on the high-latitude ozone column. When both of these forcing terms are included in the model, it is able to reproduce much of the observed year-to-year ozone variability between 1980 and 1992. Interestingly, the model indicates that there is a lot of interannual variability in the NH polar night (which is when TOMS is unable to make measurements) due to the variability in the forcing of the planetary waves.

The modeled extratropical ozone column anomaly is

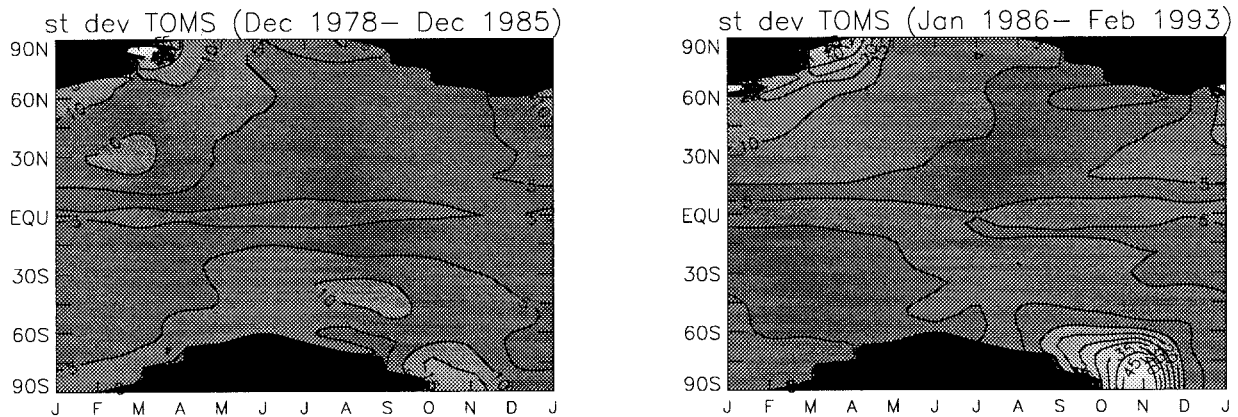


FIG. 18. As Fig. 2 but (a) from Dec 1978 to Dec 1985 and (b) from Jan 1986 to Feb 1993.

generally better correlated than observations with the Singapore wind. This is partly because the real atmosphere will not respond to the zonal wind only at a single latitude and longitude (such as over Singapore) but to the zonal wind over a range of latitudes and longitudes, and also because of the influence of other factors such as the solar cycle (e.g., McCormack and Hood 1996) and volcanic eruptions (e.g., Randel et al. 1996).

Acknowledgments. This work was supported by the National Science Foundation through Grant ATM-9526136 and by the National Aeronautics and Space Administration through Grant NAG 5-2802. We would like to thank our three reviewers for their comments.

REFERENCES

- Bowman, K. P., 1989: Global patterns of the quasi-biennial oscillation in total ozone. *J. Atmos. Sci.*, **46**, 3328–3343.
- Chandra, S., and R. S. Stolarski, 1991: Recent trends in stratospheric total ozone: Implications of dynamical and El Chichon perturbations. *Geophys. Res. Lett.*, **18**, 2277–2280.
- Chipperfield, M. P., L. J. Gray, J. S. Kinnersley, and J. Zawodny, 1994: A two-dimensional model study of the QBO signal in SAGE II NO_2 and O_3 . *Geophys. Res. Lett.*, **21**, 589–592.
- Dunkerton, T. J., and M. P. Baldwin, 1991: Quasi-biennial modulation of planetary wave fluxes in the northern hemisphere winter. *J. Atmos. Sci.*, **48**, 1043–1061.
- Garcia, R. R., and S. Solomon, 1987: A possible relationship between interannual variability in Antarctic ozone and the quasi-biennial oscillation. *Geophys. Res. Lett.*, **14**, 848–851.
- Gray, L. J., and J. A. Pyle, 1989: A two-dimensional model of the quasi-biennial oscillation of ozone. *J. Atmos. Sci.*, **46**, 203–220.
- , and T. J. Dunkerton, 1990: The role of the seasonal cycle in the quasi-biennial oscillation in ozone. *J. Atmos. Sci.*, **47**, 2429–2451.
- , and S. Ruth, 1993: The modeled latitudinal distribution of the ozone quasi-biennial oscillation using observed equatorial winds. *J. Atmos. Sci.*, **50**, 1033–1046.
- Hamilton, K., 1989: Interhemispheric asymmetry and annual synchronization of the ozone quasi-biennial oscillation. *J. Atmos. Sci.*, **46**, 1019–1025.
- Hasebe, F., 1984: The global structure of the total ozone fluctuations observed on the time scales of two to several years. *Dynamics of the Middle Atmosphere*, J. R. Holton and T. Matsuno, Eds., D. Reidel, 445–464.
- Hollandsworth, S. M., K. P. Bowman, and R. D. McPeters, 1995: Observational study of the quasi-biennial oscillation in ozone. *J. Geophys. Res.*, **100**, 7347–7361.
- Holton, J. R., and C. Mass, 1976: Stratospheric vacillation cycles. *J. Atmos. Sci.*, **33**, 2218–2225.
- , and H.-C. Tan, 1982: The quasi-biennial oscillation in the northern hemisphere lower stratosphere. *J. Meteor. Soc. Japan*, **60**, 140–147.
- Kinnersley, J. S., 1996: The climatology of the stratospheric ‘THIN AIR’ model. *Quart. J. Roy. Meteor. Soc.*, **122**, 219–252.
- , 1998: Interannual variability of stratospheric zonal wind forced by the northern lower-stratospheric large-scale waves. *J. Atmos. Sci.*, in press.
- Lait, L. R., M. R. Schoeberl, and P. A. Newman, 1989: Quasi-biennial modulation of the Antarctic ozone depletion. *J. Geophys. Res.*, **94**, 11 559–11 571.
- Lindzen, R. S., 1981: Turbulence and stress owing to gravity wave and tidal breakdown. *J. Geophys. Res.*, **86**, 9707–9714.
- McCormack, J. P., and L. L. Hood, 1996: Apparent solar cycle variations of upper stratospheric ozone and temperature: Latitude and seasonal dependences. *J. Geophys. Res.*, **101**, 20 933–20 944.
- Randel, W. J., and J. B. Cobb, 1994: Coherent variations of monthly mean total ozone and lower stratospheric temperature. *J. Geophys. Res.*, **99**, 5433–5447.
- , and F. Wu, 1996: Isolation of the ozone QBO in SAGE II data by singular-value decomposition. *J. Atmos. Sci.*, **53**, 2546–2559.
- , —, J. M. Russell III, J. W. Waters, and L. Froidevaux, 1995: Ozone and temperature changes in the stratosphere following the eruption of Mount Pinatubo. *J. Geophys. Res.*, **100**, 16 753–16 764.
- Sitnov, S. A., 1996: Vertical structure of the extratropical quasi-biennial oscillation in ozone, temperature, and wind derived from ozonesond data. *J. Geophys. Res.*, **101**, 12 855–12 866.
- Tung, K. K., 1986: Nongeostrophic theory of zonally averaged circulation. I: Formulation. *J. Atmos. Sci.*, **43**, 2600–2618.
- , and H. Yang, 1994a: Global QBO in circulation and ozone. Part I: Reexamination of observational evidence. *J. Atmos. Sci.*, **51**, 2699–2707.
- , and —, 1994b: Global QBO in circulation and ozone. Part II: A simple mechanistic model. *J. Atmos. Sci.*, **51**, 2708–2721.
- Yang, H., K. K. Tung, and E. P. Olaguer, 1990: Nongeostrophic theory of zonally averaged circulation. Part II: Eliassen–Palm flux divergence and isentropic mixing coefficient. *J. Atmos. Sci.*, **47**, 215–241.
- , and K. K. Tung, 1995: On the phase propagation of extratropical ozone quasi-biennial oscillation in observational data. *J. Geophys. Res.*, **100**, 9091–9100.
- Zawodny, J. M., and M. P. McCormick, 1991: Stratospheric Aerosol and Gas Experiment II measurements of the quasi-biennial oscillations in ozone and nitrogen dioxide. *J. Geophys. Res.*, **96**, 9371–9377.